Pharm Res
DOI 10.1007/s11095-013-1006-7

RESEARCH PAPER

Hepatocyte Nuclear Factor 4 Alpha and Farnesoid X Receptor Co-regulates Gene Transcription in Mouse Livers on a Genome-Wide Scale

Ann M. Thomas • Steve N. Hart • Guodong Li • Hong Lu • Yaping Fang • Jianwen Fang • Xiao-bo Zhong • Grace L. Guo

Received: 26 October 2012 / Accepted: 6 February 2013

ABSTRACT

Purpose Farnesoid X receptor (Fxr) is a ligand-activated nuclear receptor critical for liver function. Reports indicate that the functions of Fxr in the liver may overlap with those of hepatocyte nuclear factor 4α (Hnf4α), but studies of their precise genome-wide interaction to regulate gene transcription in the liver are lacking. Thus, we compared the genome-wide binding of Fxr and Hnf4α in the liver of mice and characterized their cooperative activity on binding to and activating target gene transcription.

Methods Genome-wide ChIP-Seq data of Fxr and Hnf4α in mouse liver were analyzed by MACS, BEDTools, and DAVID. Co-immunoprecipitation, ChIP-qPCR, and luciferase assays were done to test for protein-protein interaction and cooperative binding.

Results ChIP-seq analysis showed nearly 50% binding sites of Fxr and Hnf4α in mouse liver overlap and Hnf4α bound to shared target sites upstream and in close proximity to Fxr. Moreover, genes co-bound by Fxr and Hnf4α are enriched in complement and coagulation cascades and drug metabolism. A direct Fxr-Hnf4α protein interaction dependent on Fxr activity was detected and transcriptional assays suggest that Hnf4α can increase Fxr transcriptional activity. Conversely, binding assays showed Hnf4α can be either Fxr-dependent or -independent at different shared binding sites.

Conclusion Our results showed that Fxr cooperates with Hnf4α in the liver to modulate gene transcription. This study provides the first evidence on a genome-wide scale of both cooperative and independent interactions between Fxr and Hnf4α in regulating gene transcription in the liver.

KEY WORDS ChIP-Seq · co-regulation · Fxr · Hnf4α · nuclear receptor interaction

ABBREVIATIONS

ApoC-III	apolipoprotein C-III
CA	cholic acid
ChIP-qPCR	chromatin immunoprecipitation followed by quantitative polymerase chain reaction

Electronic supplementary material The online version of this article (doi:10.1007/s11095-013-1006-7) contains supplementary material, which is available to authorized users.

A. M. Thomas • S. N. Hart • G. Li • H. Lu • X.-b. Zhong • G. L. Guo
Department of Pharmacology, Toxicology, and Therapeutics
University of Kansas Medical Center, Kansas City, Kansas 66160, USA

A. M. Thomas
Department of Experimental Therapeutics, The University of Texas
MD Anderson Cancer Center, Houston, Texas 77054, USA

S. N. Hart
Division of Biomedical Statistics and Informatics, Mayo Clinic
Rochester, Minnesota 55905, USA

G. Li
Department of Abdominal Surgery, Cancer Treatment Center
Fourth Affiliated Hospital of Harbin Medical University
Harbin, Heilongjiang 150000, China

H. Lu
Department of Pharmacology, Upstate Medical School
Syracuse, New York 13210, USA

Y. Fang • J. Fang
Applied Bioinformatics Laboratory, Structural Biology Center
University of Kansas, Lawrence, Kansas 66047, USA

X.-b. Zhong
Department of Pharmaceutical Sciences, School of Pharmacy
University of Connecticut, Storrs, Connecticut 06269, USA

G. L. Guo (✉)
Department of Pharmacology and Toxicology, School of Pharmacy
Rutgers University, 170 Frelinghuysen Rd./EOHSI Bldg. - Rm322
Piscataway, New Jersey 08854, USA
e-mail: guo@eohsi.rutgers.edu

Published online: 06 March 2013

ChIP-Seq	chromatin immunoprecipitation followed by massively parallel sequencing
Co-IP	co-immunoprecipitation
Cyp7a1	cholesterol 7 alpha-hydroxylase
DR-1	direct hexanucleotide repeat separated by 1 nucleotide
FXR/Fxr	farnesoid X receptor
HNF4α/Hnf4α	hepatocyte nuclear factor 4 alpha
IR-1	inverted hexanucleotide repeat separated by 1 nucleotide
KO	knockout
RXRα	retinoid x receptor alpha
Shp	small heterodimer partner
Sr-b1	scavenger receptor class B type 1
TSS	transcriptional start site

INTRODUCTION

Farnesoid X receptor (FXR in humans/Fxr in rodents) is a member of the group II nuclear receptor superfamily, activated by bile acids (FXR's endogenous ligands), highly expressed in the liver and intestine, and a master regulator of the enterohepatic circulation of bile acids (1–6). Hepatocyte nuclear factor 4 alpha (HNF4α in humans/Hnf4α in rodents) is a highly conserved orphan nuclear receptor that is also essential for liver development, differentiation, and organism survival (7). Fxr and Hnf4α have been shown to regulate the expression of an overlapping set of genes, including apolipoprotein C-III (ApoC-III), cholesterol 7 alpha-hydroxylase (Cyp7a1), and bile acid-CoA:amino acid N-acyltransferase (*Baat* protein) (8–12), suggesting an overlap of Fxr and Hnf4α functions in the liver. Despite this overlap, no studies have yet determined how Fxr and Hnf4α interact in the liver on a genome-wide scale to regulate gene transcription. However, studies have shown that HNF4α is capable of enhancing the liver-specific functions of group II nuclear receptors. For example, HNF4α cooperatively enhances the transcriptional activity of constitutive androstane receptor (CAR) and pregnane X receptor (PXR) at the CYP3A4 promoter (13). The effects of HNF4α on FXR activity are largely unknown.

In addition to its role in bile acid homeostasis, Fxr also regulates other metabolic processes such as lipid homeostasis, glucose metabolism, insulin sensitivity, and gastrointestinal cancer development and therefore has become a very promising target for the treatment or prevention of cholestasis, hyperlipidemia, fatty liver, type II diabetes, liver and colon cancers (10,14–22). Recent genome-wide binding studies have shown that Fxr displays a very high degree of tissue-specific binding, which is likely regulated by other tissue-specific co-factors (23). Motif analysis of genome-wide Fxr binding in the liver revealed a nuclear receptor half site (AGGTCA) associated with the Fxr response element, an inverted repeat separated by one nucleotide (IR-1; AGGTCAnTGACCT) (23,24), indicating the involvement of orphan nuclear receptors in regulating tissue-specific functions of Fxr.

In hepatocytes, the orphan nuclear receptor HNF4α localizes mainly to the nucleus, binds DNA exclusively as a homodimer, and recognizes response elements consisting of direct repeats, namely, direct repeats separated by one nucleotide (DR-1) (25). Hnf4α regulates a myriad of liver-specific functions, including production of clotting factors, apolipoprotein synthesis, and drug metabolism (25). In addition, Hnf4α directly regulates the transcription of Cyp7a1, the rate-limiting enzyme in bile acid synthesis, suggesting that Hnf4α also plays a regulatory role in bile acid homeostasis (8,12).

Due to reports of overlapping function of Fxr and Hnf4α in liver and evidence suggesting an uncharacterized orphan nuclear receptor co-regulates the transcriptional function of Fxr, we hypothesized that Hnf4α could be responsible for mediating Fxr function in the liver. To test this theory, we compared the genome-wide binding of Fxr and Hnf4α in mouse liver and characterized these two factors' cooperation in binding to target gene regions and in activating gene transcription, using chromatin immunoprecipitation (ChIP), massive parallel sequencing, quantitative polymerase chain reaction (qPCR) analysis, co-immunoprecipitation (Co-IP) assays, and luciferase assays.

MATERIALS AND METHODS

Animals

All mice were maintained at an American Animal Associations Laboratory Animal Care-accredited facility at the University of Kansas Medical Center. Animal protocols and procedures were approved by the Institutional Animal Care and Use Committee. For Hnf4α ChIP-qPCR studies, 4-month-old fasted male wild-type (WT) and whole body Fxr–knockout (Fxr KO) (5) mice ($n=4$ per group) were used. WT mice were orally gavaged with vehicle (1% methylcellulose, 1% Triton-100 in PBS) or GW4064 (75 mg/kg) twice a day for 24 h period. GW4064 is an FXR agonist (26) synthesized by the Chemical Discovery Laboratory at the University of Kansas (Lawrence, KS). Fxr KO mice were only gavaged with vehicle. Livers were collected 4 h after the second dose and prepared for Hnf4α chromatin immunoprecipitation followed by qPCR analysis (ChIP-qPCR). Hepatocyte-specific Hnf4α-null (Hnf4α-HNull) mice were generated as previously described (27) and were fed the same rodent chow as the WT control mice. Livers from 45-day-old male Hnf4α-HNull mice and from their WT control littermates ($n=4$ per group) were used for Fxr

ChIP-qPCR assays. For Co-IP assays, 4-month-old C57BL/6 and Fxr KO mice ($n=3$ per group) we refed a control diet or a diet supplemented with 1% (*w:w*) cholic acid (CA) for 5 days. Liver whole-cell lysates were prepared and used for Co-IP analysis.

ChIP Followed by Massive Parallel Sequencing (ChIP-Seq)

ChIP-Seq analysis of Fxr and Hnf4α in mouse liver was done to determine the degree of genome-wide overlapping in binding. Original ChIP-Seq data were obtained from mouse livers generated as previously described (23,28). Raw Fxr and Hnf4αChIP-Seq data from single end sequencing on an Illumina Genome Analyzer, obtained from in-house or online databases, were re-analyzed using Model-based Analysis of ChIP-Seq (MACS) (29). Total Fxr binding sites were compared with total Hnf4α binding sites in the liver. The binding frequency of Hnf4α, or number of Hnf4α binding events, relative to the distance of the Fxr binding site within shared target genes was analyzed using BEDTools (30). Histograms of Fxr and Hnf4α binding to the *Nr0b2* (small heterodimer partner, Shp) gene were generated using the UCSC Genome Browser (University of California, Santa Cruz) (31).

Peaks identified in ChIP-Seq data that were shared by Fxr and Hnf4α in the liver of mice were analyzed for pathway enrichment using the Functional Annotation Tool in the Database for Annotation, Visualization, and Integrated Discovery (32). *P*-value less than or equal to 0.05 were considered statistically significant.

ChIP-qPCR

ChIP-qPCR analysis was done on shared Fxr and Hnfα binding regions identified by ChIP-Seq analysis to validate genome-wide analysis and to determine degree of cooperative binding of these two factors. ChIP-quality antibodies for mouse Fxr and Hnf4α were obtained from Santa Cruz Biotechnology (H-130 and C-19). Antibody specificity for Fxr has been shown in previous genome-wide binding analysis (23), and for Hnf4α is demonstrated in Supplementary Material Fig. S1. For Hnf4α ChIP-qPCR assays, we used livers from WT and Fxr KO mice treated with or without GW4064 and Fxr KO mice treated with vehicle control ($n=4$). For Fxr ChIP-qPCR assays, we used livers from WT and Hnf4α-HNull mice ($n=4$) as previously described (23). Purified IP DNA fragments were analyzed by qPCR with primers amplifying shared Fxr and Hnf4α binding sites: *Apoc3*, *Apoe*, *Baat*, *Nr0b2* promoter and 3′ regulatory region, and *Sqstm1*. We also analyzed Fxr and Hnf4α binding to fragments of genes involved in complement and coagulation cascades: *C2* (−50 to 0 bp upstream TSS), *C3* (−225 to −275 bp upstream TSS), *F2* (−425 to −475 bp upstream TSS), *C4b* (−17,125 to −17,175 bp upstream TSS), *Cfb* (−150 to −200 bp upstream TSS), *Fga* (−200 to −250 bp upstream TSS), and *Plg* (−125 to −175 bp upstream TSS). Fxr has previously been shown to bind within the second intron of the *Fgf15* gene (1,880 to 1,980 bp downstream TSS) in mouse intestine but not the liver (23). This region has also been shown not to be a binding region of Hnf4α by ChIP-Seq analysis. Therefore this region was originally used as a negative control for Fxr-Hnf4α co-localization experiments. These above target regions were selected for ChIP-qPCR validation and analysis because they belong to pathways highly co-bound by Fxr and Hnf4α, as revealed by ChIP-Seq analysis, and due to their physiologically significant roles in bile acid, lipid, and coagulation pathways. All primers used for ChIP-qPCR are presented in Supplementary Material Table SI. Quantitative PCR reactions were carried out using Maxima™ SYBR Green (Fermentas Molecular Biology Tools). Data were analyzed as fold change over values from vehicle-treated WT mice.

Co-immunoprecipitation

To investigate whether Fxr and Hnf4α have a protein–protein interaction, we used the Dynabeads Co-IP kit (Invitrogen) on whole-cell liver extracts from WT mice fed with or without 1% CA and from Fxr KO mice fed a control diet. Whole-cell lysates from mouse livers were prepared according to protocol and then immunoprecipitated using an antibody against Fxr (H-130, $n=3$ each group). Immunoprecipitates from each group were pooled and analyzed by standard Western blot using antibody sc-6556 to detect Hnf4α (Santa Cruz Biotechnology).

Construction of Plasmids for Reporter Gene Luciferase Assay

Luciferase assays were done to determine the transcriptional effects of FXR and Hnf4α on shared target regions. Specifically, the transcriptional activity of FXR/retinoid x receptor alpha (RXRα) and Hnf4α were tested on reporter vectors containing shared Fxr-Hnf4α binding regions within the promoter and the downstream regulator region of *Nr0b2* (Shp), the first intron of scavenger receptor class B type 1 (*Scarb1*; Sr-b1), and the downstream regulatory region of *Sqstm1* (p62). Supplementary Material Table SII lists the location and relative Fxr and Hnf4α binding counts in these regions. Reporter vectors of Shp promoter and downstream regulatory region were cloned as previously reported (33). An active Hnf4α binding site located 70 bp upstream of the *Baat* (Bat) gene transcriptional start site (TSS), previously reported (9), was used as a positive control for HNF4α transcriptional activity. For this study, this 600 bp region

upstream of the Bat gene, a region shown to have high Hnf4α activity (9), was amplified from mouse genomic DNA by PCR using pairs of primers containing XhoI and HindIII restriction enzyme sites and cloned upstream of the luciferase gene within the pGL4.23 firefly luciferase vector (Promega). The primers used to generate Bat reporter vector were Forward: 5′-CACAACTCGAGAATGGCTAA GACTATAGAT-3′ and Reverse: 5′-CTGAGGA AGCTTTCTTAGTATTTCCCTCCTC-3′. A 600 bp region around Fxr and Hnf4α binding sites within the first intron of Sr-b1 located 10.7 and 21.5 Kb downstream of the TSS, respectively, has been previously reported to be a Fxr binding site (34). These regions were amplified from mouse genomic DNA by PCR using pairs of primers containing XhoI and BglII restriction enzyme sites. The PCR products, Sr-b1 #1 and Sr-b1 #2, were subcloned upstream of the luciferase gene into the pGL4.23 firefly luciferase vector as previously reported (34). A 2 Kb region of the p62 gene containing Fxr and Hnf4α binding sites, located around 13.1 Kb downstream of the p62 gene TSS, has recently been determined to be an Fxr binding site (35). This region was cloned into a pGL4-TK luciferase vector (Promega) as previously reported (35). All constructs were confirmed by DNA sequencing.

Cell Culture, Transient Transfection, and Luciferase Reporter Gene Assays

Chinese hamster ovary (CHO) cells were cultured at 70–90% cell density in high-glucose Dulbecco's Modified Eagle Medium supplemented with 1% penicillin/streptomycin, 1% L-proline (50 μg/mL), and 10% fetal bovine serum (Omega Scientific) and were transiently transfected by reverse transfection methods using TurboFect (Fermentas Molecular Biology Tools) with the various reporter gene constructs as well as pCMV-ICIS human FXR and/or pCMV-SPORT6 mouse Hnf4α (Open Biosystems), PSG5 human RXRα, and phRG-TK-*Renilla*luciferase vector (Promega, no longer available; see pGL4.74) according to protocol. Human FXR is highly homologous to mouse Fxr and has often been used to test transcriptional activity on mouse gene binding sites (33,35,36). After 24 h, cells were treated with 100 nM GW4064 or 0.1% dimethyl sulfoxide (control); cells from the Hnf4α-alone groups were not treated. Firefly luciferase and *Renilla* luciferase activities were quantified 24 h post-treatment using a Dual-Glo Luciferase Assay System (Promega).

FXR/RXRα expression vectors were co-transfected with increasing amounts (3, 10, and 30 ng) of Hnf4α expression vector with 100 nM GW4064, a FXR synthetic ligand. We used the promoter and downstream regions of Shp, the intron of Sr-b1, and the downstream region of p62 cloned into luciferase expression vectors to assess the effects of Hnf4α on the transcriptional activity of FXR. The transcriptional activity of increasing amounts of Hnf4α expression vector (10, 50, and 100 ng or 10 and 100 ng) on these regions, as well as on a positive control gene, Bat, were also measured by luciferase assay. The firefly luciferase activity value was normalized as a ratio over *Renilla* luciferase and expressed as firefly luciferase activity/*Renilla*. The data are presented as the average of six wells ± SE, and the experiments were repeated at least twice.

Statistical Analysis

All data are presented as mean ± SE. Statistical difference between the two groups was analyzed by Student's *t*-test. *P*-values≤0.05 were considered significant.

RESULTS

Genome-Wide Fxr and Hnf4α Binding Sites in Mouse Liver

ChIP-Seq binding data of Fxr and Hnf4α in mouse liver from previous reports (23,28) were re-analyzed using MACS. We found 10,917 total binding sites for Hnf4α and 7,797 for Fxr, of which 3,882 overlap; 50% of total Fxr binding sites co-localize with Hnf4α (Fig. 1a). Hnf4α and Fxr do not bind to same site; rather, the frequency (y-axis) of Hnf4α binding to shared target genes was greatest when bound upstream and in close proximity to an Fxr binding site (x-axis; location of collective Fxr binding sites are represented by "0"; Fig. 1b).

Pathway analysis of shared Fxr and Hnf4α target genes revealed pathways involving complement and coagulation cascades had the highest number of genes targeted by Fxr and Hnf4α (Table I). *P*-values and Bonferonni scores illustrate the degree of significance of Fxr and Hnf4α co-localization within the pathway. *P*-values≤0.05 were considered statistically significant. Table II lists the shared target genes categorized by the Kyoto Encyclopedia of Genes and Genomes pathway maps as part of complement and coagulation cascades, the locations of Fxr and Hnf4α binding sites in relation to the genes' TSS and the relative binding events (counts) of each factor.

Fig. 1c is a histogram of binding of Fxr (red) and Hnf4α (black) to the *Nr0b2* gene in mouse liver, generated by the UCSC Genome Browser (31). Both the promoter and downstream FXR binding sites co-localized with those of HNF4α. The binding of Hnf4α to the *Nr0b2* promoter has previously been described (37). However, the binding of Hnf4α to the 3′ end of the *Nr0b2* gene and the co-localization with Fxr at these regions are novel findings. Sequence analysis of these regions by NUBIScan (38) showed

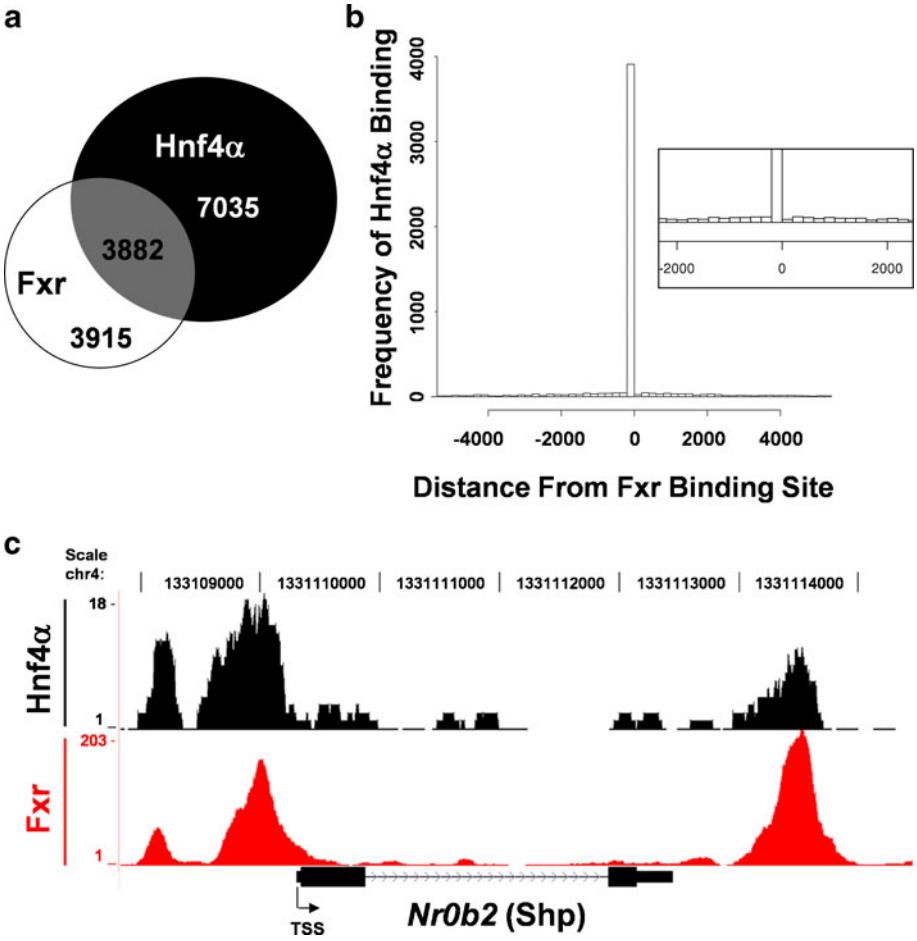

Fig. 1 Genome-wide binding of Fxr and Hnf4α in mouse liver. Previously reported Fxr and Hnf4α ChIP-Seq data was reanalyzed using MACS (23,28). (**a**) Venn diagram of total Hnf4α and Fxr binding sites in mouse liver as revealed by chromatin immunoprecipitation followed by massively parallel sequencing (ChIP-Seq) analysis. We found 10,917 total Hnf4α binding sites and 7,797 total Fxr binding sites in mouse liver, of which 3,882 (nearly 50%) overlapped. (**b**) Histogram of the binding frequency, or number of binding events, of Hnf4α (y-axis) in relation to distance from the Fxr binding site (x-axis) to the shared target genes in mouse liver. Collective Fxr binding sites are represented by "0". (**c**) Histogram of Fxr (*red*) and Hnf4α (*black*) binding to the *Nr0b2* (Shp) gene in mouse liver as determined by ChIP-Seq analysis. This histogram was generated using the UCSC Genome Browser (University of California, Santa Cruz).

a putative HNF4α binding motif, DR-1, located in the promoter of the *Nr0b2* gene (within −320 to −220 bp upstream of TSS) but not in the downstream regulatory region (data not shown), whereas a classical FXR binding motif, IR-1, has been identified in both of these regions (23,33).

Dependence of Fxr and Hnf4α for Binding to Shared Target Genes

Supplementary Material Table SII summarizes the binding site locations and counts of Fxr and Hnf4α to select shared target genes, including to the 5′ and 3′ end of *Nr0b2*, revealed by ChIP-Seq analysis. These regions were assessed for Fxr and Hnf4α binding by ChIP-qPCR and luciferase assay. Fxr binding increased nearly 2-fold in Hnf4α-HNull mice at sites located within the *Baat* gene promoter, the 5′ and 3′ regions of the *Nr0b2* gene, the downstream regulatory region of *Sqstm1* gene, and a non-shared target site within the *Fgf15* gene (Fig. 2a). This increase was only statistically significant for Fxr binding at the 5′ end of *Nr0b2* and *Fgf15* (**P*-value≤ 0.05). *Fgf15* was thought to be an FXR target gene in mouse intestine and not liver (23), and was shown to not be bound by Hnf4α. This region was originally used as a negative control region for co-localization. The increased binding of Fxr to this region is an interesting observance discussed further in the discussion. Fxr binding to promoters of *Apoc3* and *Apoe* did not change with Hnf4α deficiency.

We also analyzed Fxr binding to genes involved in complement and coagulation cascades (Fig. 2b) in WT *versus* Hnf4α-HNull mouse liver. Fxr did bind to shared regions in genes of the complement and coagulation cascade within both WT and Hnf4α-HNull mouse liver. Fxr binding events increased in Hnf4α-deficient mice 1.6–2-fold at genes *Fga*, *C3*, *C4b*, *C2*, and *F2* but did not change at binding sites within *Cfb* and *Plg*.

The Hnf4α binding pattern to shared target genes in WT mouse liver treated with or without Fxr ligand GW4064 and in Fxr KO mouse liver, varied at different target sites (Fig. 3). When compared with vehicle-treated WT liver, Hnf4α binding events in WT mice treated with GW4064 increased at shared target sites within *Apoc3* (1.5-fold), *Apoe* (2.3-fold), *Baat* (1.8-fold), *Nr0b2* (1.6- and 1.5-fold), and *Sqstm1* (1.5-fold) but not in the negative control region (*Fgf15*) (Fig. 3a; **P*-value<0.05). Overall, Hnf4α binding to *Apoe*, *Baat*, *Nr0b2* 5′, and *Sqstm1* regions did not decrease below baseline in Fxr KO mouse livers. There was a slight non-significant reduction in *Apoc3*

Table I Pathways Enriched by Both Fxr and Hnf4α Binding in Mouse Liver

Pathway	Genes[a]	% bound by Fxr and Hnf4α	*P*-Value	Bonferroni
Complement and coagulation cascades	17	2.24	1.38E-07	2.25E-05
Drug metabolism	16	2.11	8.33E-07	1.36E-04
PPAR signaling pathway	16	2.11	1.67E-06	2.73E-04
Metabolism of xenobiotics by cytochrome P450	13	1.71	2.97E-05	4.83E-03
Insulin signaling pathway	12	1.58	4.55E-02	0.999
Glycine, serine and threonine metabolism	9	1.18	6.15E-05	9.97E-03
Steroid hormone biosynthesis	9	1.18	7.58E-04	0.116
Adipocytokine signaling pathway	9	1.18	9.80E-03	0.799
Pyruvate metabolism	8	1.05	2.07E-03	0.287
Fatty acid metabolism	8	1.05	3.59E-03	0.443
Drug metabolism	8	1.05	5.19E-03	0.572
Retinol metabolism	8	1.05	3.20E-02	0.995
Cysteine and methionine metabolism	7	0.92	3.10E-03	0.397
Linoleic acid metabolism	7	0.92	1.61E-02	0.929
Biosynthesis of unsaturated fatty acids	6	0.79	6.32E-03	0.644
Starch and sucrose metabolism	6	0.79	2.13E-02	0.97
ABC transporters	6	0.79	4.99E-02	1
Selenoamino acid metabolism	5	0.66	1.80E-02	0.948
Alanine, aspartate and glutamate metabolism	5	0.66	4.36E-02	0.999
Primary bile acid biosynthesis	4	0.53	2.74E-02	0.989

[a] the number of genes bound by FXR and Hnf4α in this pathway

binding, and binding to *Nr0b2* 3′ remained elevated in Fxr KO mouse liver. Hnf4α binding increased in mouse liver treated with GW4064 at genes *F2* (2.6-fold), *C2* (1.6-fold), *C4b* (1.7-fold), *C3* (1.4-fold), and *Cfb* (1.9-fold) (Fig. 3b; **P*-value≤0.05). As seen with the previous regions above, Hnf4α binding to *F2*, *C3*, and *Cfb* did not decrease below baseline in FxrKO mouse liver. However, Hnf4α binding remained elevated at regions within *C2* and *C4b* (***P*-value≤0.05). Hnf4α binding was not regulated by Fxr activity at binding sites within *Plg* or *Fga*.

Table II List of Target Genes Within Complement and Coagulation Cascades Bound by Both Fxr and Hnf4α

Official gene symbol	Binding site location from TSS	Fxr total counts[a]	Hnf4α total counts[a]
Plg	−144, 1,992, 6,986, 9,608	99, 155, 127, 95	46, 39, 31, 33
Fga	−225, −5,561	150, 105	40, 53
Cpb2	−9,013, 9	52, 34	38, 19
Serpina1e	−4,534, 3,769	76, 35	62, 27
Fgg	−345, −4,534, 1,904, 2,607	70, 197, 20, 28	9, 47, 26, 25
F2	−436	129	67
Mbl1	−44, 9,558	192, 156	24, 64
Cfh	21	109	21
Kng2	−125, −10,481	69, 40	39, 17
Serpine1	−507	115	33
Cfb	−183	217	78
Serpinf2	−66	41	22
C4b	−17,142	93	83
C2	−4	68	46
C3	−236, −2,276, −2,788, −5,187	884, 75, 69, 175	46, 15, 10, 55
Proc	−1,366	77	53
Kng1	−124, −1,946	96. 24	35, 21

[a]counts are the number of binding events recorded for Fxr and HnfF4α at each location

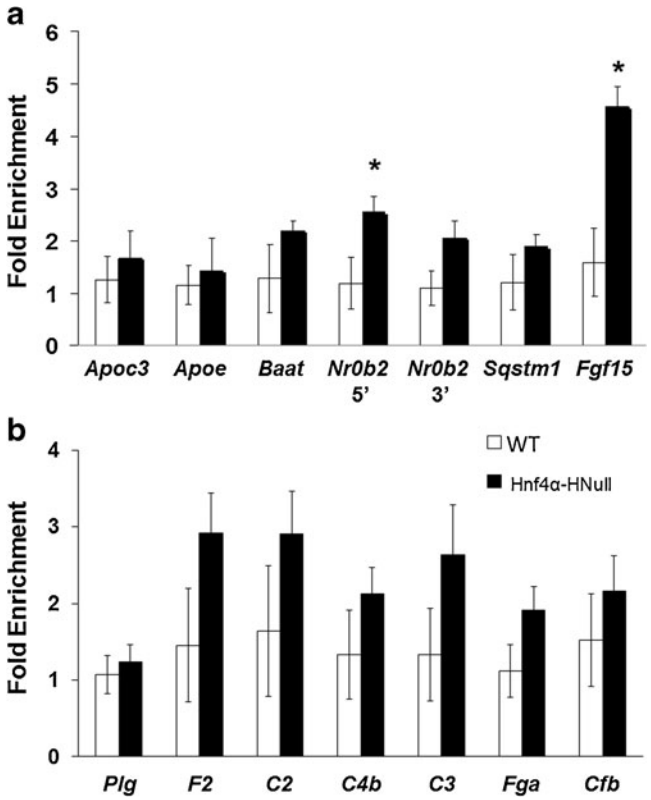

Fig. 2 ChIP-qPCR analysis of Fxr binding to shared target genes. QPCR analysis was performed on DNA fragments immunoprecipitated with Fxr antibody. ChIP-qPCR data are reported as fold increase (y-axis) of Fxr binding in Hnf4α-HNull (*black bar*) mouse liver compared to WT (*white bar*) mouse liver. **P*-value≤0.05. (**a**) ChIP-qPCR results of Fxr binding to shared target regions in WT and Hnf4α-HNull mouse liver. Regions within the *Apoc3* promoter, the *Apoe* promoter, the *Baat* promoter, the promoter and 3′ region of *Nr0b2*, and downstream of the *Sqstm1* TSS are shared target sites of Fxr and Hnf4α as revealed by ChIP-Seq analysis of mouse liver (Supplementary Material Table SII). *Fgf15* is a target gene of Fxr (but not Hnf4α) in the intestine but not the liver and therefore was originally used as a negative control. (**b**) ChIP-qPCR results of Fxr binding to shared target regions of genes categorized within complement and coagulation cascades in WT and Hnf4α-HNull mouse liver. These binding sites are located within the promoters (within 500 bp upstream of TSS) of *Plg*, *F2*, *C2*, *C3*, *Fga*, *Cfb*, and −17,125 to −17,175 bpupstream of *C4b* gene TSS (Table II).

Interaction Between Fxr and Hnf4α and Dependence of FXR and Hnf4α for Activating Target Genes

A modest Fxr-Hnf4α protein–protein interaction was detected in WT mice fed a control diet (Fig. 4a). This interaction increased in mice fed a 1% CA diet but was nearly undetectable in Fxr KO mice (Fig. 4a).

Hnf4α binding to Shp promoter and downstream regulatory region was detected by ChIP-Seq analysis (Fig. 2a). These binding sites were analyzed for Hnf4α transcriptional activity using luciferase reporter assays. Transcriptional activity of Hnf4α on the Bat gene promoter, which has already been characterized (9), served as a positive control. Results showed that although Hnf4α significantly increased luciferase activities of the Shp and Bat promoter when compared to vector control, with 100 ng Hnf4α having the highest activity (**P*-value≤0.05), Hnf4α did not affect the downstream regulatory region of Shp (Fig. 4b, top panel).

FXR has previously been shown to transcriptionally regulate the promoter and downstream regulatory region of the Shp gene (33). Our results confirm that FXR significantly increases luciferase activity at both of these sites (**P*-value≤ 0.05; Fig. 4b, bottom panel). In addition, Hnf4α increased transcriptional activity of FXR on Shp 3′ region nearly 2- and 1.4 fold (***P*-value≤0.05) at 3 and 10 ng. However, Hnf4α appears to have slightly and significantly decreased transcriptional activity of FXR at the Shp promoter (***P*-value≤0.05).

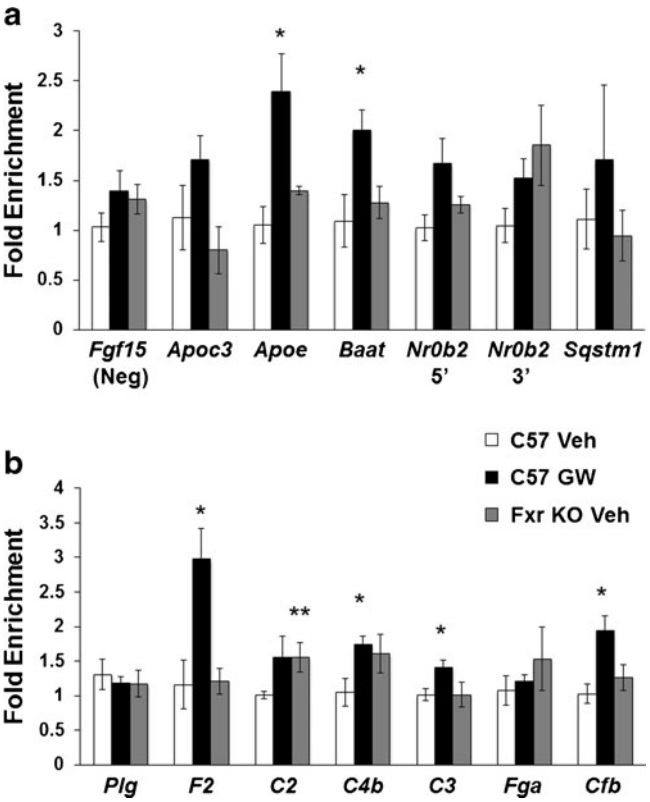

Fig. 3 ChIP-qPCRof Hnf4α binding to shared target genes. (**a**) Fxr shares the Hnf4α binding regions within the *Apoc3* promoter, the *Apoe* promoter, the *Baat* promoter, the promoter and 3′ region of *Nr0b2*, and downstream of the *Sqstm1* TSS, revealed by ChIP-qPCR (Supplementary Material Table SII). The *Fgf15* binding site was determined not to be an Hnf4α binding site and therefore was used as a negative control. Hnf4α binding to these regions was investigated in WT and Fxr KO vehicle and WT GW4064 treated mouse liver. Data are reported as fold enrichment (y-axis) of Hnf4α binding in WT GW (*black bar*) or Fxr KO veh (*gray bar*) treated mouse liver normalized to WT veh (*white bar*) treated mouse liver. (**b**) ChIP-qPCR data of Hnf4α binding to shared target regions within genes categorized as part of complement and coagulation cascade. These binding sites are located within the promoters (within 500 bp upstream of TSS) of *Plg*, *F2*, *C2*, *C3*, *Fga*, *Cfb*, and −17,125 to −17,175 bp upstream of *C4b* gene TSS (Table II). Data are reported as described in part (**a**). **P*-value≤ 0.05 of C57 GW treated group compared to C57 veh group. ***P*-value≤ 0.05 in Fxr KO vehicle group compared to C57 veh group.

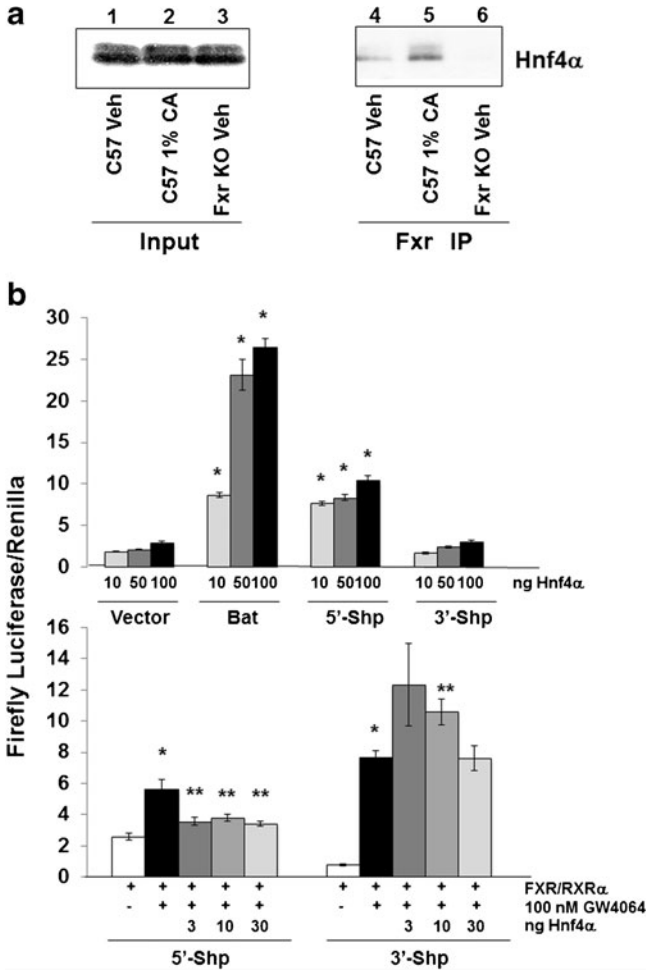

Fig. 4 Co-IP of Fxr and Hnf4α and luciferase assays of Shp regulatory regions. (**a**) Co-IP of WT mice fed control or 1% CA diet and Fxr KO mice fed control diet. Whole cell liver lysates were prepared and immunoprecipitated using an antibody against Fxr. Liver lysates (input) and IP fractions were pooled and analyzed by Western blot analysis using antibody against Hnf4α. Lanes 1–3 show the levels of Hnf4α within 15 μg of pooled whole-cell lysates from WT control diet (Lane 1), WT 1% CA diet (Lane 2), and Fxr KO control diet (Lane 3) groups. Lane 4–6 show levels of Hnf4α detection within WT control diet (Lane 4), WT 1% CA diet (Lane 5), and Fxr KO control diet (Lane 6) liver lysates immunoprecipitated with an Fxr antibody. (**b**) Luciferase expression assays showing the effects of increasing amounts of mouse Hnf4α expression vector (10, 50, 100 ng) on transcriptionally activating regulatory regions within the Bat gene promoter, the 5′ and 3′ regulatory regions of the Shp gene, or the luciferase vector control (top panel). Bottom panel shows the effects of increasing mouse Hnf4α expression vector amounts (3, 10, and 30 ng) on FXR-induced transcription of the 5′ and 3′ regulatory regions of the Shp gene after activation of FXR with 100 nM of GW4064. Results are reported as a ratio of firefly luciferase activity over *Renilla* luciferase activity (y-axis). **P*-value ≤ 0.05 of Hnf4α transfected groups when compared to vector or FXR/RXRα GW treated groups compared to veh control. ***P*-value ≤ 0.05 of Hnf4α transfected GW treated groups compared to FXR/RXRα alone GW treated groups.

Hnf4α significantly reduced luciferase activity of the Sr-b1#1 (10.7 Kb regulatory region downstream of the TSS, Supplementary Material Table SII), 2-fold for 10 ng and 1.3-fold for 100 ng of Hnf4α expression vector (**P*-value ≤ 0.05; Fig. 5a top). Conversely, Hnf4α significantly increased luciferase activity of the Sr-b1#2 site (21.5 Kb regulatory region downstream of the TSS, Supplementary Material Table SII) and p62 (**P*-value ≤ 0.05 at 100 ng for Sr-b1 #2 and at 10 and 100 ng for p62; Fig. 5a middle and bottom). Next, the effects of Hnf4α on FXR transcriptional activity of binding sites within Sr-b1 and p62 were tested (Fig. 5b). FXR significantly increased transcriptional activity of two binding sites within the Sr-b1gene (#1 and #2) and downstream regulatory region of p62 (**P*-value ≤ 0.05), which is consistent with previous reports (34,35). Hnf4α increased FXR-induced transcriptional activity at each of these sites. Interestingly, even though Hnf4α alone moderately decreased luciferase activity at Sr-b1#1 (Fig. 5a, top), Hnf4α synergistically and significantly enhanced the FXR activity nearly 20-fold in this region at 30 ng of Hnf4α expression vector (***P*-value ≤ 0.05 for 3 and 30 ng; Fig. 5b, top). Hnf4α only moderately enhanced FXR's transcriptional activity at Sr-b1 #2 in a weakly additive and dose-dependent manner (***P*-values ≤ 0.05; Fig. 5b, middle). Finally, Hnf4α significantly enhanced FXR transcriptional activity of p62, although this effect was saturated at 3 ng of Hnf4α expression vector and again was weakly additive (***P*-value ≤ 0.05 for 3 and 30 ng; Fig. 5b, bottom). Collectively, these results indicate that Hnf4α can enhance FXR activity in an additive and synergistic manner.

DISCUSSION

Our findings demonstrate that genome-wide Hnf4α and Fxr DNA-binding sites have a very high degree of overlap in mouse liver and that these shared target genes are highly enriched within the genes involved in complement and coagulation cascades. Furthermore, within shared target regions, these two nuclear receptors bind in close proximity and exhibit a protein–protein interaction dependent on Fxr activation. Deficiency of Fxr or Hnf4α affects the binding of either to target genes in a gene-selective manner. We conclude that Fxr and Hnf4α likely regulate transcription of some shared target genes independently of each other, as seen with apolipoprotein genes, but cooperate to regulate transcription of other shared target genes, such as genes involved in bile acid homeostasis.

There are several potential explanations for why Fxr binding increases at select shared target genes in the absence of functional Hnf4α, which is opposite to the original hypothesis. Hnf4α and Fxr may compete for the same binding site to regulate transcription of the target gene, as illustrated in previous studies showing that Fxr displaces Hnf4α binding to the Apo C-III promoter and inversely regulates transcription of this gene (10). However, in the current study, ChIP-Seq analysis on a genome-wide scale shows Hnf4α

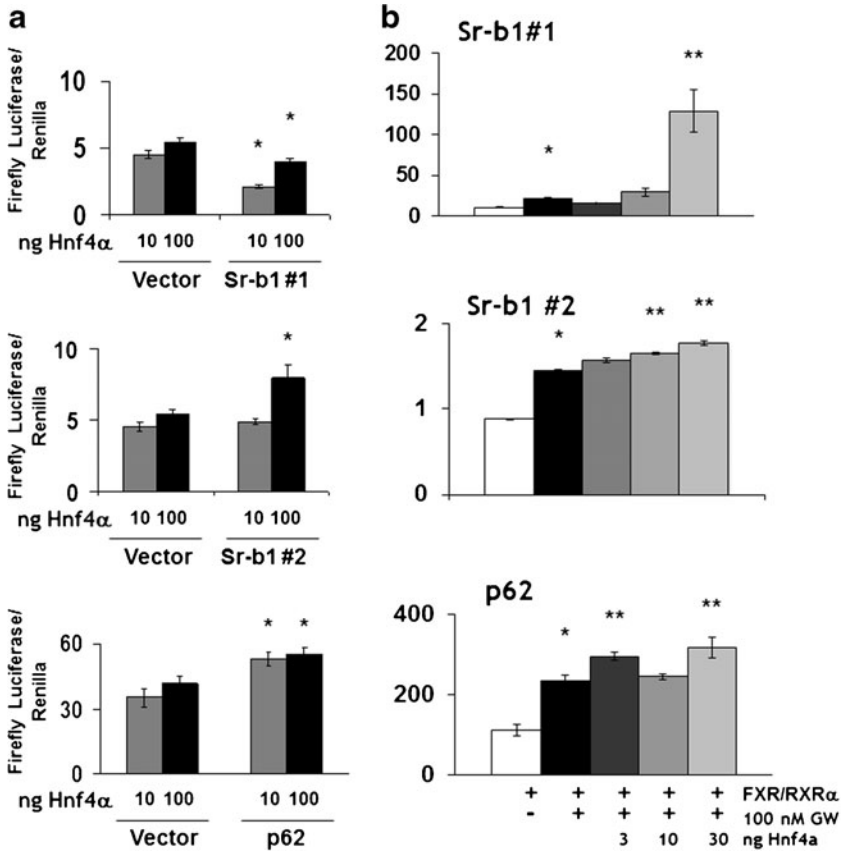

Fig. 5 Transcriptional effects of Hnf4α alone and with FXR at shared target genes by luciferase assays. (**a**) Luciferase expression assays showing the effects of increasing amounts Hnf4α expression vector (10 and 100 ng) on transcriptionally activating regulatory regions within 10.6 Kb (#1; top) and 21.5 Kb (#2; middle) downstream of the Sr-b1 TSS, in the downstream regulatory region of p62 (bottom), and in the luciferase vector controls. (**b**) Effects of increasing amounts of Hnf4α expression vector (3, 10, and 30 ng) on FXR-induced transcription of regulatory regions within the Sr-b1 gene (#1 (*top*) and #2 (*middle*)) and p62 (*bottom*) after activation of FXR with 100 nM of GW4064. Results of luciferase assays (both **a** and **b**) are reported as a ratio of firefly luciferase activity over *Renilla* luciferase activity (y-axis). **P*-value ≤ 0.05 of Hnf4α transfected groups when compared to vector or FXR/RXRα GW treated groups compared to veh control. ***P*-value ≤ 0.05 of Hnf4α transfected GW treated groups compared to FXR/RXRα alone GW treated groups.

binding not at the same location as Fxr but rather upstream of the Fxr binding site. We think that increased FXR binding is due to the increase in endogenous ligands of Fxr in the Hnf4α mice, because loss of Hnf4α leads to a marked increase in bile acid concentration (8,9), which likely further activates Fxr. This is illustrated by the increase in Fxr binding within a region of *Fgf15*, which is not typically an Fxr target gene in the liver under normal conditions. Therefore, our results suggest complex interactions among nuclear receptors via direct interaction at the chromatin level or via the modification of endogenous ligands.

Furthermore, we found that increased Hnf4α binding to shared target genes depended on Fxr activity at some target regions, including the promoter of the *Baat* gene and the 3′ regulatory region of *Nr0b2*. Interestingly, baseline binding of Hnf4α to the 3′ end of the *Nr0b2* gene increased in Fxr KO mice compared with WT mice. This trend was also seen at *C4b* and *C2*. This observance possibly indicates the ability of Hnf4α to compensate for the loss of FXR at these regions. The dependence of Hnf4α binding on Fxr activity within complement and coagulation genes also showed differential regulation. Indeed, Hnf4α binding increased at binding sites within *F2*, *C2*, *C3*, *C4b*, and *Cfb* genes, but not at *Plg* or *Fga* genes, after Fxr activation. The increased binding at these five regions was shown to depend on the activation of Fxr at *F2*, *C3*, and *Cfb*. The mechanism responsible for the differential binding of Hnf4α in the absence of Fxr is unknown but could be due to direct modification of Hnf4α binding to chromatin, post-translational modification of Hnf4α, a change in Hnf4α ligand availability, and/or as mentioned, the compensation of Hnf4α for Fxr loss. Further studies will be needed to clarify the underlying mechanism.

Similarly, transcriptional assays indicated that Hnf4α binding detected by ChIP-Seq analysis is not directly correlated to transcriptional regulation of genes. For example, Hnf4α showed a low level of binding to the 3′ end of the *Nr0b2* gene as well as to sites 10.7 Kb downstream of the Sr-b1 TSS. However, neither of these sites was transcriptionally activated by Hnf4α. Although Hnf4α alone did not elicit transcription of these sites, it did moderately enhance FXR's

transcriptional activity in both of these regions, suggesting that Hnf4α regulates FXR activity or other factors, possibly via modifying the chromatin structure. Furthermore, Hnf4α alone induced transcriptional activity of the *Nr0b2* promoter but seemed to have a slight, insignificant inhibitory effect on FXR's transcriptional activity in this region.

Future studies will determine whether HNF4α interacts with FXR to stabilize localized chromatin environments surrounding gene loci. A recent study has shown that Fxr binding to the 5′ and 3′ end of *Nr0b2* mediates a head-to-tail chromatin loop around the gene (33). This may be an essential process required for the efficient transcription of the *Nr0b2* gene in response to Fxr activation. ChIP-Seq data demonstrates that Hnf4α also co-localizes with Fxr to the 5′ and 3′ regions of *Nr0b2*, suggesting that Hnf4α may be important for mediating the Fxr-induced head-to-tail chromatin loop around the *Nr0b2* gene.

Other studies have demonstrated that Fxr and Hnf4α have opposite effects on gene transcription of shared target genes. Studies show that Hnf4α binding increases the transcription of ApoC-III, a well-characterized Hnf4α target gene (11,39). Conversely, Fxr inhibits the transcription of ApoC-III by binding to its promoter region (10). However, none of these studies have examined the transcriptional effect of Hnf4α and Fxr on shared targets genes on a genome-wide scale. Our analysis suggests these two factors can have cooperative, compensatory, or independent effects on the transcription of target genes. In addition, although not completely demonstrated here, these factors can have an antagonistic effect on gene transcription as previously reported (10).

It is interesting to note that the degree of induction in binding in experimental groups was small or lacked statistical significance. We have seen increasing numbers of genes being regulated in this way despite strong binding of transcription factors (TFs) revealed by ChIP-Seq analysis (23), and due to valid negative control comparisons, we do not believe this to be a result of false positive binding. One explanation for this observance could be the inability of antibody-TF interactions from experimental technology to enrich small fractions of desired TF-DNA interactions from whole tissues. Furthermore, previous publications from our group have reported a similar phenomenon with Fxr (23). In this study, it was argued due to potential constitutive TF binding; ligand activation of the TF does not necessarily result in increased localization of TF to target DNA, but rather changes the recruitment of co-repressors to co-activators.

Nevertheless, this study provides the first line of evidence for interactions between Fxr and other nuclear receptors on a genome-wide scale in mouse liver. FXR and HNF4α have been shown to be highly homologous between mouse and human (36,40), and have similar functions between these species (41). Therefore, information gained from these mouse models will likely reveal similar FXR-HNF4α interactions in human. It was originally thought that HNF4α could regulate FXR activity similar to how forkhead box protein A1 (FOXA1), otherwise known as hepatocyte nuclear factor 3-alpha, directs estrogen receptor alpha genome-wide binding (42,43). However, this study revealed a more complex Fxr-Hnf4α interaction in mouse liver that was both Fxr-dependent and -independent, illustrated an indirect cross-talk resulting from disruption of bile acid homeostasis in Fxr and Hnf4α deficient mice, and implicated chromatin remodeling as a mechanism of cooperative activity between these two factors. These studies help broaden our understanding of nuclear receptor function and the complicated interactions they have with other transcriptional machinery that is necessary to fine-tune target gene transcription.

CONCLUSION

In summary, our results reveal a high percentage of co-localized Fxr binding to Hnf4α in mouse liver. We conclude that Fxr and Hnf4α cooperate to a moderate extent to regulate gene transcription and share a direct protein interaction. They likely regulate transcription of target genes in both a dependent and independent manner and can cooperate or antagonize the activity of the other. Our findings suggest that both factors can compensate for the other's deficiency at certain sites and this compensation may be a mechanism important for maintaining cellular integrity and homeostasis. Despite a direct Fxr-Hnf4α interaction, it is unlikely that Hnf4α is a major determining orphan nuclear receptor responsible for directing tissue-specific binding of Fxr. Nonetheless, the Fxr-Hnf4α interaction could play a critical role in certain diseased systems and/or within specific cellular pathways such as complement and coagulation cascades or drug metabolism and should be further investigated.

ACKNOWLEDGMENTS AND DISCLOSURES

This work was supported by CPRIT Training Grants RP101502 to The University of Texas MD Anderson Cancer Center (AMT), DK031343 (GLG), DK090036 (GLG), and a Madison and Lila Self Graduate Fellowship from the University of Kansas (SNH).

REFERENCES

1. Parks DJ, Blanchard SG, Bledsoe RK, Chandra G, Consler TG, *et al.* Bile acids: natural ligands for an orphan nuclear receptor. Science. 1999;284:1365–8.
2. Makishima M, Okamoto AY, Repa JJ, Tu H, Learned RM, *et al.* Identification of a nuclear receptor for bile acids. Science. 1999;284:1362–5.

3. Wang H, Chen J, Hollister K, Sowers LC, Forman BM. Endogenous bile acids are ligands for the nuclear receptor Fxr/Bar. Mol Cell. 1999;3:543–53.
4. Seol W, Choi HS, Moore DD. Isolation of proteins that interact specifically with the retinoid X receptor: two novel orphan receptors. Mol Endocrinol. 1995;9:72–85.
5. Sinal CJ, Tohkin M, Miyata M, Ward JM, Lambert G, *et al.* Targeted disruption of the nuclear receptor Fxr/Bar impairs bile acid and lipid homeostasis. Cell. 2000;102:731–44.
6. Kok T, Hulzebos CV, Wolters H, Havinga R, Agellon LB, *et al.* Enterohepatic circulation of bile salts in farnesoid X receptor-deficient mice. J Biol Chem. 2003;278:41930–7.
7. Chen WS, Manova K, Weinstein DC, Duncan SA, Plump AS, *et al.* Disruption of the Hnf-4 gene, expressed in visceral endoderm, leads to cell death in embryonic ectoderm and impaired gastrulation of mouse embryos. Genes Dev. 1994;8:2466–77.
8. Inoue Y, Yu AM, Yim SH, Ma X, Krausz KW, *et al.* Regulation of bile acid biosynthesis by hepatocyte nuclear factor 4alpha. J Lipid Res. 2006;47:215–27.
9. Inoue Y, Yu AM, Inoue J, Gonzalez FJ. Hepatocyte nuclear factor 4alpha is a central regulator of bile acid conjugation. J Biol Chem. 2004;279:2480–9.
10. Claudel T, Inoue Y, Barbier O, Duran-Sandoval D, Kosykh V, *et al.* Farnesoid X receptor agonists suppress hepatic apolipoprotein Ciii expression. Gastroenterology. 2003;125:544–55.
11. Shih DQ, Dansky HM, Fleisher M, Assmann G, Fajans SS, *et al.* Genotype/phenotype relationships in Hnf-4alpha/Mody1: haploinsufficiency is associated with reduced apolipoprotein (Aii), apolipoprotein (Ciii), lipoprotein (a), and triglyceride levels. Diabetes. 2000;49:832–7.
12. Stroup D, Chiang JY. Hnf4 and Coup-Tfii interact to modulate transcription of the cholesterol 7alpha-hydroxylase gene (Cyp7a1). J Lipid Res. 2000;41:1–11.
13. Tirona RG, Lee W, Leake BF, Lan LB, Cline CB, *et al.* The orphan nuclear receptor Hnf4alpha determines Pxr- and car-mediated xenobiotic induction of Cyp3a4. Nat Med. 2003;9:220–4.
14. Zhang Y, Lee FY, Barrera G, Lee H, Vales C, *et al.* Activation of the nuclear receptor Fxr improves hyperglycemia and hyperlipidemia in diabetic mice. Proc Natl Acad Sci U S A. 2006;103:1006–11.
15. Watanabe M, Houten SM, Wang L, Moschetta A, Mangelsdorf DJ, *et al.* Bile acids lower triglyceride levels via a pathway involving Fxr, Shp, and Srebp-1c. J Clin Invest. 2004;113:1408–18.
16. Staels B, Kuipers F. Bile acid sequestrants and the treatment of type 2 diabetes mellitus. Drugs. 2007;67:1383–92.
17. Cariou B, van Harmelen K, Duran-Sandoval D, van Dijk TH, Grefhorst A, *et al.* The farnesoid X receptor modulates adiposity and peripheral insulin sensitivity in mice. J Biol Chem. 2006;281:11039–49.
18. Ma K, Saha PK, Chan L, Moore DD. Farnesoid X receptor is essential for normal glucose homeostasis. J Clin Invest. 2006;116:1102–9.
19. Maran RR, Thomas A, Roth M, Sheng Z, Esterly N, *et al.* Fxr deficiency in mice leads to increased intestinal epithelial cell proliferation and tumor development. J Pharmacol Exp Ther. 2009;328:469-77.
20. Modica S, Murzilli S, Salvatore L, Schmidt DR, Moschetta A. Nuclear bile acid receptor Fxr protects against intestinal tumorigenesis. Cancer Res. 2008;68:9589–94.
21. Kim I, Morimura K, Shah Y, Yang Q, Ward JM, *et al.* Spontaneous hepatocarcinogenesis in farnesoid X receptor-null mice. Carcinogenesis. 2007;28:940–6.
22. Yang F, Huang X, Yi T, Yen Y, Moore DD, *et al.* Spontaneous development of liver tumors in the absence of the bile acid receptor farnesoid X receptor. Cancer Res. 2007;67:863–7.
23. Thomas AM, Hart SN, Kong B, Fang J, Zhong XB, *et al.* Genome-wide tissue-specific farnesoid X receptor binding in mouse liver and intestine. Hepatology. 2010;51:1410–9.
24. Chong HK, Infante AM, Seo Y-K, Jeon T-I, Zhang Y, *et al.* Genome-wide interrogation of hepatic Fxr reveals an asymmetric Ir-1 motif and synergy with Lrh-1. Nucleic Acids Res. 2010;38:6007–17.
25. Gonzalez FJ. Regulation of hepatocyte nuclear factor 4 alpha-mediated transcription. Drug Metab Pharmacokinet. 2008;23:2–7.
26. Maloney PR, Parks DJ, Haffner CD, Fivush AM, Chandra G, *et al.* Identification of a chemical tool for the orphan nuclear receptor Fxr. J Med Chem. 2000;43:2971–4.
27. Hayhurst GP, Lee YH, Lambert G, Ward JM, Gonzalez FJ. Hepatocyte nuclear factor 4alpha (nuclear receptor 2a1) is essential for maintenance of hepatic gene expression and lipid homeostasis. Mol Cell Biol. 2001;21:1393–403.
28. Schmidt D, Wilson MD, Ballester B, Schwalie PC, Brown GD, *et al.* Five-vertebrate Chip-Seq reveals the evolutionary dynamics of transcription factor binding. Science. 2010;328:1036–40.
29. Zhang Y, Liu T, Meyer CA, Eeckhoute J, Johnson DS, *et al.* Model-based analysis of Chip-Seq (Macs). Genome Biol. 2008;9:R137.
30. Quinlan AR, Hall IM. Bedtools: a flexible suite of utilities for comparing genomic features. Bioinformatics. 2010;26:841–2.
31. Kent WJ, Sugnet CW, Furey TS, Roskin KM, Pringle TH, *et al.* The human genome browser at UCSC. Genome Res. 2002;12:996–1006.
32. Dennis Jr G, Sherman BT, Hosack DA, Yang J, Gao W, *et al.* David: database for annotation, visualization, and integrated discovery. Genome Biol. 2003;4:P3.
33. Li G, Thomas AM, Hart SN, Zhong X, Wu D, *et al.* Farnesoid X receptor activation mediates head-to-tail chromatin looping in the Nr0b2 gene encoding small heterodimer partner. Mol Endocrinol. 2010;24:1404–12.
34. Li G, Thomas AM, Williams JA, Kong B, Liu J, *et al.* Farnesoid X receptor induces murine scavenger receptor class B type I via intron binding. PLoS One. 2012;7:e35895.
35. Williams JA, Thomas AM, Li G, Kong B, Zhan L, *et al.* Tissue specific induction of P62/Sqstm1 by farnesoid X receptor. PLoS One. 2012;7:e43961.
36. Huber RM, Murphy K, Miao B, Link JR, Cunningham MR, *et al.* Generation of multiple farnesoid-X-receptor isoforms through the use of alternative promoters. Gene. 2002;290:35–43.
37. Li T, Chiang JY. Rifampicin induction of Cyp3a4 requires pregnane X receptor cross talk with hepatocyte nuclear factor 4alpha and coactivators, and suppression of small heterodimer partner gene expression. Drug Metab Dispos. 2006;34:756–64.
38. Podvinec M, Kaufmann MR, Handschin C, Meyer UA. Nubiscan, an in silico approach for prediction of nuclear receptor response elements. Mol Endocrinol. 2002;16:1269–79.
39. Sladek FM, Zhong WM, Lai E, Darnell Jr JE. Liver-enriched transcription factor Hnf-4 is a novel member of the steroid hormone receptor superfamily. Genes Dev. 1990;4:2353–65.
40. Bolotin E, Schnabl JM, Sladek FM, in Yusuf D *et al.* Hnf4a: the transcription factor encyclopedia. Genome Biol. 2012;13:R24.
41. Modica S, Gadaleta RM, Moschetta A. Deciphering the nuclear bile acid receptor Fxr paradigm. Nucl Recept Signal. 2010;8:e005.
42. Hurtado A, Holmes KA, Ross-Innes CS, Schmidt D, Carroll JS. Foxa1 is a key determinant of estrogen receptor function and endocrine response. Nat Genet. 2011;43:27–33.
43. Lupien M, Eeckhoute J, Meyer CA, Wang Q, Zhang Y, *et al.* Foxa1 translates epigenetic signatures into enhancer-driven lineage-specific transcription. Cell. 2008;132:958–70.